

A Multivariate Training Technique with Event Reweighting

Hai-Jun Yang*, Tiesheng Dai, Alan Wilson, Zhengguo Zhao, Bing Zhou

Department of Physics, University of Michigan, Ann Arbor, MI 48109-1120, USA

**E-mail: yhj@umich.edu*

ABSTRACT: An event reweighting technique incorporated in multivariate training algorithms has been developed and tested with Artificial Neural Networks (ANN) and Boosted Decision Trees (BDT). The performance of the ANNs and BDTs resulting from this event reweighting training is compared to the performance from conventional equal event weighting training. The comparison is performed in the context of physics analysis in the ATLAS experiment at the Large Hadron Collider (LHC), which will explore the fundamental nature of matter and the basic forces that shape our universe. We demonstrate that the event reweighting technique provides an unbiased method of multivariate training for event pattern recognition.

KEYWORDS: Pattern Recognition, cluster finding, calibration and fitting methods; Analysis and Statistical methods.

Contents

| | |
|--|----------|
| 1. Introduction | 1 |
| 2. MC Samples and Training Variables | 2 |
| 3. Event Reweighting Training Technique | 5 |
| 3.1 BDT Reweighting | 5 |
| 3.2 ANN Reweighting | 6 |
| 4. Application and Results | 7 |
| 5. Uncertainty Studies | 8 |
| 6. Conclusions | 9 |
| 7. Acknowledgments | 9 |

1. Introduction

Artificial Neural Networks (ANN) and Boosted Decision Trees (BDT) [1, 2, 3, 4, 5, 6] are two important data analysis tools that have wide application in High Energy Physics experiments for particle identification and for event pattern recognition [7, 8, 9, 10]. Both methods 'train' the 'networks' or the 'trees' based on a set of 'signal' and 'background' features (physical quantities) to obtain a powerful discriminant variable that distinguishes signal from background. This process is called 'event pattern recognition' in physics data analysis. In the conventional ANN and BDT algorithms for high energy physics analysis, the training events (including signal and background) are initialized with equal weights. The equal event weight training technique works fine if the Monte Carlo (MC) samples from different physics processes used for training are generated based on their production rates. In physics studies, we need to have very large MC 'background' event samples to determine the rates of the misclassified events from different processes that contaminate the signal (normally a few times more MC data than real data is needed for a certain integrated luminosity). However, for hadron colliders such as the Large Hadron Collider at CERN (LHC, <http://cern.ch/>) and Tevatron at Fermilab (<http://www.fnal.gov/>), it is unrealistic and inefficient to generate MC data for all the physics processes with full detector simulations based on their production rates. This is simply because of limited CPU time and data storage capacity. To simulate and reconstruct an event for the ATLAS experiment, typically, it would take about 10 minutes of CPU time and about 2.5 MB of storage space per event. The simulation time is many orders of magnitude longer than the event created from the beam collisions.

Combining statistically limited MC events from different physics processes raises a natural question on the multivariate training process in event weighting. Suppose that 100K MC events are generated for each of background A and background B. Suppose, in addition, we expect 80% of the background to be from A and 20% from B. What is proposed in the event reweighting technique is that the events are reweighted for training, so that 80% of the total weight is from A and 20% is from B, i.e. each event from A has 4 times the weight as an event from B. We implemented this idea in ANN and BDT training programs and tested this technique in the context of the ATLAS experiment with fully simulated MC datasets.

ATLAS (<http://atlas.web.cern.ch/>) is one of two general purpose detectors at the LHC (a 27 km circumference particle accelerator that will collide protons head-on with a center of mass energy of 14 TeV) being built at the European Center for Nuclear Research (CERN) in Geneva, Switzerland. The ATLAS experiment is designed to search for signals that would respond to the electroweak symmetry breaking. Some theoretic models predicted signals such as standard model Higgs bosons, supersymmetric particles, and new bosons from extra dimensions. Discovering any one of those signals at the LHC would be a great breakthrough in our understanding of particle physics. The LHC will begin operation in 2008. A major part of preparing for LHC physics analysis is to develop and test advanced data analysis tools.

In this paper, we use ATLAS MC samples for $WZ \rightarrow \ell\nu\ell\ell$ analysis to demonstrate that using event reweighting technique will provide an unbiased training in ANN and BDT multivariate analysis. Our 'signal' is from the WZ triple-lepton decay channels ($ee\nu\nu$, $ee\mu\nu$, $\mu\mu\nu\nu$ and $\mu\mu\mu\nu$). Major backgrounds come from standard model processes such as $t\bar{t}$, $Z + jets$, ZZ and $Drell - Yan$. Those backgrounds have production rates 3-4 orders of magnitude larger than that of the signal process. Our goals are to maximize signal efficiency, to minimize background efficiency and to understand the uncertainties with limited training and test samples.

For comparing the performance of the ANN and the BDT with or without event reweighting training, we used the same testing sample (statistical independent of training sample). The main purpose of this paper is to compare the training performance with and without event reweighting. Performance comparisons between ANN and BDT can be found in the contexts of MiniBooNE neutrino oscillation analysis[2, 4], D0 single top discovery[9] and B-tagging[10].

In section 2 we provide the MC signal and background information, including the physics processes, the production cross-sections at the LHC, the total simulated MC event size and the training sample size after pre-selection. We also give brief descriptions of physics variables for both the ANN and the BDT analysis. The event reweighting training techniques for BDT and ANN are presented in section 3. Performance comparisons for different weighting methods are summarized in section 4. Section 5 presents uncertainty study results and section 6 gives our conclusions.

2. MC Samples and Training Variables

Monte Carlo samples used in this study are from the ATLAS Computing System Commissioning (CSC) [11] with full detector simulation and reconstruction. For this study we used a few loose cuts to pre-select events with the approximate experimental signature of the signal, then the pre-selected events are analyzed using the ANN and BDT multivariate programs to further separate signal from

background events. In Table 1 we list the MC and pre-selection information for the signal (WZ) and background MC events used in this study. This information includes the total production cross-sections (σ_{MC}) [12], the triple-lepton decay branching ratio (Br), the total number of simulated MC events (N_{MC}), the number of pre-selected events (N_{precut}), and the number of expected events (N_{exp}) normalized to 1 fb^{-1} integrated luminosity ($\int Ldt$) after the pre-selection. The initial event weight for each process is listed in Table 1 as well. The cross-section correction factor, K , in the Table 1 is defined as the ratio of the next-to-leading order (NLO) cross-section to the cross-section obtained from the MC generators. Thus, if we used a NLO MC generator, the K value is 1. Otherwise, if a LO MC generator is used, the K value is $\sigma(NLO)/\sigma(LO)$ (σ denotes the cross-section). The expected number of events for 1 fb^{-1} , N_{exp} , and the event's *weight* listed in Table 1 are calculated based on

$$N_{exp} = \frac{\sigma_{MC} \times K \times Br \times (\int Ldt) \times N_{precut}}{N_{MC}}$$

and

$$Weight = \frac{\sigma_{MC} \times K \times Br \times (\int Ldt)}{N_{MC}}.$$

The integrated luminosity ($\int Ldt$) is a constant (1 fb^{-1}) for all the MC process, so the event weight of a given MC process depends on its production cross-section, decay branching ratio and the total number of MC events generated (N_{MC}). For a given MC process, a larger event weight means lower statistics for analysis. In general, higher MC statistics are desired to reduce statistical uncertainty for data analysis. Evidently, the event weights vary dramatically among the various MC processes as shown in Table 1.

The pre-selection applied loose cuts to all datasets by requiring two leptons with invariant mass consistent with the Z mass and an additional lepton with missing transverse energy forming a transverse mass consistent with the W boson mass. The pre-selection also requires that at least one lepton have transverse momentum greater than 20 GeV to satisfy the trigger requirements of the experiment.

The physics variables input into the ANN and BDT trainings are selected based on our experience with cut-based analysis (optimized to separate signal from background), and the variable 'Gini' index determined from the decision trees [2]. This index indicates the separation power between signal and background of a variable. We give brief descriptions of these variables, separated into four categories.

- **Energy and Momentum**

The characteristics of energy and momentum are different from the WZ events and the background events. For example, $t\bar{t}$ events will have larger hadronic jet energies compared to the WZ events, the $Z + X$ background will have lower missing transverse energy and so on. The energy and momentum variables we used are

- P_T^ℓ - lepton transverse momentum, three variables (two leptons decay from Z, one lepton decays from W),
- MET - missing transverse energy,
- MET significance which is defined as $MET / \sqrt{\sum_i E_T(i)}$, (i is the index counting leptons and jets),

- E_T^h - vector sum of transverse momentum from leptons and MET ,
- H_t - scalar sum of transverse momentum from jets, leptons and MET ,
- $\sum E_T^{jet}$ - sum of transverse energy from each jet,
- $P_T(WZ)$ - transverse momentum of WZ bosons,
- E_T^{recoil} - total recoil transverse energy.

• Lepton isolations

The leptons from the W and Z decays are isolated, but leptons from the QCD jets are not isolated. Typically, the QCD jets have multiple tracks and larger energy deposition around the leptons. The isolation variables we used are

- N_{trk}^{iso} - number of charged tracks in $\Delta R < 0.4$ cone around a lepton ($\Delta R = \sqrt{(\Delta\phi)^2 + (\Delta\eta)^2}$), three variables (two leptons decay from Z , one lepton decays from W),
- $\sum P_T^{iso}$ - sum of track P_T in a $\Delta R < 0.4$ cone around a lepton,
- $\sum E_T^{iso}$ - sum of jet transverse energy in $\Delta R < 0.4$ cone around a lepton,
- f_ℓ^{iso} - fraction of energy = $[E(\Delta R < 0.4) - E(\Delta R < 0.2)] / E_T^\ell$.

• Event topologies

The following variables are selected to suppress top and QCD jet events and to separate fake lepton events from the WZ signal:

- $\Delta R(\ell, \ell')$ - separation between two leptons, 2 variables (one lepton decays from W , the other lepton decays from Z),
- ΔA - vertex difference between leptons in transverse plane (impact parameter), 2 variables (one lepton decays from W , the other lepton decays from Z).

• Mass information

The mass information is used to reduce QCD and $t\bar{t}$ background events with leptons (or fake leptons) that do not decay from Z and W . Two variables are used in our analysis:

- $M_{\ell\ell}$ - invariant mass of two leptons from Z decays,
- $M_T(\ell, MET)$ - transverse mass of a lepton and MET (neutrino) from W decays.

For variable distribution shape comparisons, we show some energy and momentum variable distributions for signal and background in Figure 1 and some variable distributions related to lepton isolation, event topology and mass in Figure 2. All the events in the plots are passed pre-selection cuts and each signal (black histograms) and background distribution is normalized to the same area.

Figure 3 and 4 show the same variable distributions with event weighting. In these plots, the background histograms are stacked, with areas reflecting the relative weights. For comparison, total background events and total signal events are normalized to the same area, respectively.

From the variable distributions (both for signal and background), we found that a single variable has limited power to separate signal from background. But, when combining these variables using ANN or BDT, the signal and background could be well separated, particularly when the proper event reweighting algorithm is used in the multivariate analysis.

The BDT program provides a sensitive measure to indicate the signal and background separation effectiveness of each input variable based on the Gini index contribution [2]. We list the Gini index contributions of the input variables in our analysis for both event reweighting and equal weighting cases in Table 2. For each variable, a larger Gini index indicates a relatively larger contribution to the overall signal to background separation. From the Gini index listed in this table we know that the lepton isolation and mass variables are especially effective at separating the WZ signal from various background events. However, for equal weighting training, the BDT algorithm tends to focus on separating the WZ signal from the ZZ background mainly because the ZZ events dominate the background training sample after the pre-selection.

3. Event Reweighting Training Technique

As we mentioned in Section 2, the event weights of various MC processes are quite different. MC samples with larger event weights represent lower statistics relative to cross-section and vice versa. For instance, the MC $pp \rightarrow ZZ \rightarrow \ell\ell\ell\ell$ sample has a total of 35700 events (before the pre-selection). A total cross section of 18860 fb (NLO) and a four-lepton decay branching ratio of 0.0045 means that for 1 fb^{-1} integrated luminosity the total number of expected $ZZ \rightarrow \ell\ell\ell\ell$ is about 85. Thus, the ZZ event weight is 0.0024, as listed in Table 1. In contrast, the Drell-Yan sample at the Z mass ($pp \rightarrow Z(\ell^+\ell^-)(M_Z = 81 - 100 \text{ GeV})$) contains 3.28 million events and yet the NLO cross-section and branching ratio indicate that 1.85 times as many events (6.05 million) are expected in 1 fb^{-1} integrated luminosity, thus this sample has a weight of 1.85.

If we treat these MC events from different sources equally using conventional training techniques, then multivariate training methods for ANNs and BDTs will focus disproportionately on the MC events with lower event weights. This is because those events have a higher probability of being selected for the ANN training relative to their rate of production in the experiment. In the BDT training process, a sample with larger statistics relative to cross-section will have relatively larger total event weight. This will affect which variables are chosen to be split in the tree and the value at which the splitting cut occurs. For example, in our analysis undue emphasis would be put on the variables separating the ZZ background from signal. To avoid this training prejudice we used event reweighting for the ANN and BDT training. As illustrated above, the event weights for different physics processes are independent of pre-selection as shown in the Weight definition expression in section 2 and Table 1. As will be described in the following subsections, the sums of all the weights of training signal or background events after pre-selection are normalized to 1.

3.1 BDT Reweighting

In the BDT training process we start with N_s pre-selected signal and N_{bg} pre-selected background events. In the traditional BDT algorithm[2, 3] using equal event weighting for training, the initial weights of signal and background events are N_s^{-1} and N_{bg}^{-1} , respectively. The total signal event weight and the total background event weight are each normalized to 1. We implement the event reweighting training technique for BDT by initializing the weights of all the training events to the event weights ($WT_s(i), i = 1, 2, \dots, N_s$ for signal events; $WT_{bg}(i), i = 1, 2, \dots, N_{bg}$ for background events) listed in Table 1, then we normalize the total signal event weight and the total background

event weight each to 1. For signal events, the initial weight for BDT training is

$$wt_s(i) = WT_s(i)/WTOT_s, i = 1, 2, \dots, N_s,$$

where

$$WTOT_s = \sum_{i=1}^{N_s} WT_s(i).$$

For background events, the initial weight for BDT training is

$$wt_{bg}(j) = WT_{bg}(j)/WTOT_{bg}, j = 1, 2, \dots, N_{bg},$$

where

$$WTOT_{bg} = \sum_{j=1}^{N_{bg}} WT_{bg}(j).$$

In our analysis, we have used the ϵ -boost algorithm [2] with $\epsilon = 0.01$. For the BDT training we used 1000 tree iterations and 20 terminal leaves per decision tree.

3.2 ANN Reweighting

For conventional ANN training both signal and background events are selected randomly with the same probability for each training iteration. This is the equal event weighting training technique. When we have multiple sources of background events with different production cross-sections from the proton-proton collisions the equal event weighting training technique may not work well, particularly when the number of background events in the training sample are not proportional to the production cross-sections. Effectively, the background events with large cross-section are underrepresented, and don't receive appropriate training. So, we developed the event reweighting algorithm to improve the training process for ANN. The basic idea of the event reweighting technique is to modify the probability of a given event to be selected for the ANN training. For all the MC events, the reweighting (determination of the probability) should be automatically included in the ANN program, which reflects the weights of the underlying physics. We briefly describe our algorithm below.

Suppose we have three different background samples, A, B and C. These samples have N_A , N_B and N_C events, respectively. Based on production cross-sections and the pre-selection efficiencies, we expect the background contributions from sample A, B, and C are 50%, 30% and 20% respectively. Thus, sample A events should have 50% probability to be selected for training, sample B and C should have 30% and 20% probabilities to be selected for training, respectively. So, the probabilities of selecting a single training event in background samples A, B and C are $50\%/N_A$, $30\%/N_B$ and $20\%/N_C$, respectively.

The general algorithm, as implemented in the code is the following,

- start with weights of training signal and background events listed in Table 1, $wt(j)$, $j = 1, 2, \dots, N_i$ (i = signal or background),
- calculate accumulated weights for event j , $wt_sum(j)$:
 $wt_sum(j) = wt_sum(j-1) + wt(j)$, $j = 2, \dots, N$,

- generate a random number with uniform distribution in a range of $[0, wt_sum(N)]$,
- select an event for the ANN training by minimizing the generated random number R_n and the accumulated weight $wt_sum(i)$: $\min |R_n - wt_sum(i)|$, $i = 1, \dots, N$,
- iterate the above process many times for the ANN training.

The event reweighting training technique can be applied to various ANN algorithms. For this analysis, we used a back-propagation neural network with three layers, one input, one hidden and one output layer. There are 22 nodes in both the input and hidden layers, and there is one output node. The neuron response is a sigmoid function. The learning rate is $\eta = 0.05$, the momentum is $\alpha = 0.07$ and 1,000,000 training cycles are used for the ANN training. The general description of the ANN can be found in section 6.8 of the TMVA User guide[1].

4. Application and Results

The MC signal $WZ \rightarrow \ell\nu\ell\ell$ and all the background pre-selected events are split into two nearly equal samples. Odd and even numbered events in each MC process are grouped into sample A and B, respectively. Sample A and B are statistically independent. We use sample A for training and then use sample B for testing.

The training sample had 5983 signal and 7907 background events. The testing sample had 5983 signal and 7894 background events. We performed the ANN and the BDT analysis by using equal weight and reweighting techniques. We show both results in Figure 5 and Figure 6. The results shown in these plots are for the testing sample. Figure 5 shows the ANN analysis results and Figure 6 shows the BDT results. In both figures, the top plots show the analysis with the event reweighting technique and the bottom plots show results with the equal weight technique. In those plots, the solid histograms are for the signal and the dotted histograms are for the backgrounds. Both signal and backgrounds are normalized to 1 fb^{-1} integrated luminosity.

As we expected, the signal events are mainly distributed in an area close to 1 in the ANN output spectrum, and the background events are distributed close to 0 (see Figure 5). The top plot of Figure 5, the ANN output spectrum produced with the reweighting algorithm, shows that the signal distribution is much sharper around an ANN output of 1. However, with equal weight training, the signal distribution near 1 is smeared out. As a result, the signal selection efficiency decreases significantly when using conventional technique of training with equal weights.

Similarly, we observed in Figure 6 that the BDT output with event reweighting training has much better signal to background separation power (top plot) compared to that with equal weighting event training (bottom plot).

By choosing the selection cuts on the ANN or the BDT output spectra, we can determine the number of selected signal and background events as well as the experimental signal to background ratio. Our comparison of the analysis performance using different training techniques focuses on the relative difference between signal and background, thus we look at the number of selected signal events versus background events as the selection cut varies.

Comparisons of reweighting and equal weighting techniques with the ANN and BDT analyses are shown in Figure 7, where we plot the expected number of background events versus the

number of signal events corresponding to an integrated luminosity of 1 fb^{-1} by varying the ANN and the BDT output selection cuts. The black solid curve represents results from the BDT with event reweighting for training; the red dashed curve shows results from the BDT with equal event weighting; the green dotted curve indicates results from the ANN with event reweighting; and, the blue dash-dotted curve shows results from the ANN with equal event weighting for training. From these curves we see that, for the same number of signal events selected using ANN or BDT, using the event reweighting technique gives much lower background event contamination compared to equal event weighting.

The numerical comparisons are shown in Table 3. We vary the selection cuts on the ANN and BDT output spectra to keep the same number of signal events and then compare the background contamination and the ratio of background contamination determined from reweighting and equal event weighting techniques. Our analysis shows that, compared with the equal weighting training, the ANN and BDT trained with event reweighting reduce the background by factors of about $5 \sim 7$ and $6 \sim 10$, respectively.

5. Uncertainty Studies

The reweighting technique will rely on our knowledge of the event production rates (cross-sections) in the colliders. Thus, it is important to understand the multivariate training stability with respect to the production cross-section uncertainties of the MC processes. We looked at BDT training to estimate these effects. We introduced 20% uncertainties to the event weights for our training samples, while for the testing sample we have kept the 'correct' event weights. Compared with the original BDT performance without cross-section uncertainties, the relative changes of the BDT performance with 20% cross-section uncertainties are less than about 6%, e.g. while keeping the same number of signal events, the background contamination increased by 4-7% depending on cuts. This uncertainty is well within the 15-25% relative Root-Mean-Squared (RMS) errors of background efficiencies which will be described below.

Generally, a large training sample is desired for training in multivariate algorithms. It is important to understand what is a sufficient number of training events such that the background efficiency is insensitive to training sample size. To this end, we studied the background efficiencies and RMS errors as a function of the number of training events for a set of fixed signal efficiencies as shown in Figure 8. The training events are selected randomly with replacement from the training sample with 5983 signal and 7907 background events for the BDT training, and a statistically independent MC sample with 5983 signal and 7894 background events is used for testing. For each training point, the BDT training-testing process is repeated 50 times with a different set of training samples and a fixed testing sample to obtain the average background efficiencies and RMS errors for a given set of signal efficiencies. Figure 8 indicates that fewer MC events for training will result in larger background contaminations, presumably because the number of MC events is insufficient to fully train the BDTs. We also note that with at least 10000 training events the background efficiency becomes relatively stable. We have used about 14000 events for training, thus we expect the bias due to training sample size should be small.

6. Conclusions

We have developed and tested an event reweighting technique to be used when training multivariate pattern recognition processes. This technique is necessary to train the pattern recognition in an unbiased way, particularly for multi-background processes with limited MC statistics. For the ATLAS $WZ \rightarrow \ell\nu\ell\ell$ analysis, with large background contributions from different physics processes, we found that for good performance using the ANN and the BDT analysis one should employ event reweighting in the training process.

7. Acknowledgments

We wish to express our gratitude to the ATLAS Collaboration for their excellent work on the Monte Carlo simulation and physics analysis software. We also would like to thank Byron P. Roe and Ji Zhu for useful discussions. This work is supported by the Department of Energy (DE-FG02-95ER40899) of the United States.

References

- [1] A. Hocker et.al., *TMVA - Toolkit for Multivariate Data Analysis* [physics/0703039].
- [2] Byron P. Roe, Hai-Jun Yang, Ji Zhu, Yong Liu, Ion Stancu, Gordon McGregor, *Boosted decision trees as an alternative to artificial neural networks for particle identification*, *Nucl. Instrum. & Meth. A* **543** (2005) 577 [physics/0408124].
- [3] Hai-Jun Yang, Byron P. Roe, Ji Zhu, *Studies of boosted decision trees for MiniBooNE particle identification*, *Nucl. Instrum. & Meth. A* **555** (2005) 370 [physics/0508045].
- [4] Hai-Jun Yang, Byron P. Roe, Ji Zhu, *Studies of Stability and Robustness for Artificial Neural Networks and Boosted Decision Trees*, *Nucl. Instrum. & Meth. A* **574** (2007) 342 [physics/0610276].
- [5] Y. Freund and R.E. Schapire (1996), *Experiments with a new boosting algorithm*, *Proc COLT*, 209–217. ACM Press, New York (1996).
- [6] J. Friedman, *Greedy function approximation: a gradient boosting machine*, *Annals of Statistics*, **29**(5), (2001) 1189-1232; J. Friedman, T. Hastie, R. Tibshirani, *Additive Logistic Regression: a Statistical View of Boosting*, *Annals of Statistics*, **28**(2), (2000) 337-407
- [7] The MiniBooNE Collaboration, A.A. Aguilar-Arevalo et.al., *A Search for electron neutrino appearance at the $\Delta m^2 \sim 1 \text{ eV}^2$ scale*, *Phys. Rev. Lett.* **98**, (2007) 231801 [hep-ex/0704.1500]
- [8] The BABAR Collaboration, B. Aubert et.al., *Measurement of CP-violating asymmetries in the $B^0 \rightarrow K^+ K^- K^0$ Dalitz plot*, [hep-ex/0607112].
- [9] The D0 Collaboration, V.M. Abazov et.al., *Evidence for Production of Single Top Quarks and First Direct Measurement of $|V_{tb}|$* , *Phys. Rev. Lett.* **98**, (2007) 181802.
- [10] J. Bastos, Y. Liu, *A multivariate approach to heavy flavour tagging with cascade training*, *JINST* **2**, (2007) P11007
J. Bastos, *Tagging heavy flavors with boosted decision trees*, [physics/0702041].
- [11] <https://twiki.cern.ch/twiki/bin/view/Atlas/CSCNotesList>
<https://twiki.cern.ch/twiki/bin/view/Atlas/CSCDistributedProduction>

| MC Process | $\sigma_{MC}(\text{fb})$ | K | Br | N_{MC} | N_{precut} | N_{exp}/fb^{-1} | Weight |
|--|--------------------------|-----|--------|----------|--------------|-------------------|--------|
| $pp \rightarrow W^+ Z \rightarrow \ell^+ \nu \ell^+ \ell^-$ | 0.3673E+05 | 1.0 | 0.0144 | 26550 | 6848 | 136.4 | 0.0199 |
| $pp \rightarrow W^- Z \rightarrow \ell^- \bar{\nu} \ell^+ \ell^-$ | 0.2099E+05 | 1.0 | 0.0144 | 17450 | 5118 | 88.7 | 0.0173 |
| $pp \rightarrow Z/\gamma \rightarrow \ell^+ \ell^-$ | 0.8910E+06 | 1.5 | 0.0672 | 999742 | 111 | 10.0 | 0.0898 |
| $pp \rightarrow Z(e^+e^-) + jet(E_{jet} = 10 - 20 \text{ GeV})$ | 0.1360E+08 | 1.3 | 0.0336 | 597281 | 0 | 0.0 | 0.9946 |
| $pp \rightarrow Z(e^+e^-) + jet(E_{jet} = 20 - 40 \text{ GeV})$ | 0.8670E+07 | 1.3 | 0.0336 | 398697 | 0 | 0.0 | 0.9499 |
| $pp \rightarrow Z(e^+e^-) + jet(E_{jet} = 40 - 80 \text{ GeV})$ | 0.4120E+07 | 1.3 | 0.0336 | 397524 | 0 | 0.0 | 0.4527 |
| $pp \rightarrow Z(e^+e^-) + jet(E_{jet} = 80 - 120 \text{ GeV})$ | 0.8270E+06 | 1.3 | 0.0336 | 397009 | 0 | 0.0 | 0.0910 |
| $pp \rightarrow Z(e^+e^-) + jet(E_{jet} > 120 \text{ GeV})$ | 0.3830E+06 | 1.3 | 0.0336 | 198652 | 0 | 0.0 | 0.0842 |
| $pp \rightarrow Z(\tau^+\tau^-) + jet(E_{jet} = 10 - 20 \text{ GeV})$ | 0.1360E+08 | 1.3 | 0.0336 | 598783 | 0 | 0.0 | 0.9921 |
| $pp \rightarrow Z(\tau^+\tau^-) + jet(E_{jet} = 20 - 40 \text{ GeV})$ | 0.8670E+07 | 1.3 | 0.0336 | 399076 | 0 | 0.0 | 0.9490 |
| $pp \rightarrow Z(\tau^+\tau^-) + jet(E_{jet} = 40 - 80 \text{ GeV})$ | 0.4120E+07 | 1.3 | 0.0336 | 398972 | 0 | 0.0 | 0.4511 |
| $pp \rightarrow Z(\tau^+\tau^-) + jet(E_{jet} = 80 - 120 \text{ GeV})$ | 0.8270E+06 | 1.3 | 0.0336 | 396671 | 0 | 0.0 | 0.0911 |
| $pp \rightarrow Z(\tau^+\tau^-) + jet(E_{jet} > 120 \text{ GeV})$ | 0.3830E+06 | 1.3 | 0.0336 | 199046 | 0 | 0.0 | 0.0840 |
| $pp \rightarrow Z(\mu^+\mu^-) + jet(E_{jet} = 10 - 20 \text{ GeV})$ | 0.1360E+08 | 1.3 | 0.0336 | 2996413 | 492 | 97.5 | 0.1983 |
| $pp \rightarrow Z(\mu^+\mu^-) + jet(E_{jet} = 20 - 40 \text{ GeV})$ | 0.8670E+07 | 1.3 | 0.0336 | 1995792 | 789 | 149.7 | 0.1898 |
| $pp \rightarrow Z(\mu^+\mu^-) + jet(E_{jet} = 40 - 80 \text{ GeV})$ | 0.4120E+07 | 1.3 | 0.0336 | 1189793 | 1516 | 229.3 | 0.1513 |
| $pp \rightarrow Z(\mu^+\mu^-) + jet(E_{jet} = 80 - 120 \text{ GeV})$ | 0.8270E+06 | 1.3 | 0.0336 | 397856 | 1105 | 100.3 | 0.0908 |
| $pp \rightarrow Z(\mu^+\mu^-) + jet(E_{jet} > 120 \text{ GeV})$ | 0.3830E+06 | 1.3 | 0.0336 | 199832 | 1133 | 94.9 | 0.0837 |
| $pp \rightarrow Z(\ell^+\ell^-)(M_Z = 30 - 81 \text{ GeV})$ | 0.4220E+07 | 1.3 | 0.1010 | 1000000 | 16 | 8.9 | 0.5541 |
| $pp \rightarrow Z(\ell^+\ell^-)(M_Z = 81 - 100 \text{ GeV})$ | 0.4610E+08 | 1.3 | 0.1010 | 3284999 | 406 | 748.1 | 1.8426 |
| $pp \rightarrow Z(\ell^+\ell^-)(M_Z > 100 \text{ GeV})$ | 0.1750E+07 | 1.3 | 0.1010 | 971000 | 271 | 64.1 | 0.2366 |
| $pp \rightarrow Z\mu\mu (M_{inv} > 150 \text{ GeV})$ | 0.1750E+07 | 0.8 | 0.0336 | 43000 | 33 | 36.1 | 1.0940 |
| $pp \rightarrow Z\mu\mu Jet$ | 0.8270E+06 | 0.8 | 0.0336 | 35000 | 20 | 12.7 | 0.6351 |
| $pp \rightarrow Zee (Pt > 100 \text{ GeV})$ | 0.8270E+06 | 0.8 | 0.0336 | 46000 | 11 | 5.3 | 0.4833 |
| $pp \rightarrow Z\mu\mu (Pt > 100 \text{ GeV})$ | 0.8270E+06 | 0.8 | 0.0336 | 33000 | 42 | 28.3 | 0.6736 |
| $pp \rightarrow Z\tau\tau (Pt > 100 \text{ GeV})$ | 0.8270E+06 | 0.8 | 0.0003 | 32000 | 41 | 0.3 | 0.0069 |
| $pp \rightarrow t\bar{t}$ | 0.7590E+06 | 1.0 | 0.5550 | 604750 | 1071 | 746.0 | 0.6966 |
| $pp \rightarrow Z\gamma (Pt > 25 \text{ GeV})$ | 0.4510E+05 | 1.0 | 0.0672 | 46800 | 43 | 2.8 | 0.0648 |
| $pp \rightarrow W^+ W^- \rightarrow e^+ \nu e^- \bar{\nu}$ | 0.1133E+06 | 1.0 | 0.0120 | 41950 | 9 | 0.3 | 0.0324 |
| $pp \rightarrow W^+ W^- \rightarrow e^+ \nu \mu^- \bar{\nu}$ | 0.1133E+06 | 1.0 | 0.0120 | 45900 | 22 | 0.7 | 0.0296 |
| $pp \rightarrow W^+ W^- \rightarrow e^+ \nu \tau^- \bar{\nu}$ | 0.1133E+06 | 1.0 | 0.0120 | 71000 | 7 | 0.1 | 0.0191 |
| $pp \rightarrow W^+ W^- \rightarrow \mu^+ \nu e^- \bar{\nu}$ | 0.1133E+06 | 1.0 | 0.0120 | 47000 | 18 | 0.5 | 0.0289 |
| $pp \rightarrow W^+ W^- \rightarrow \mu^+ \nu \mu^- \bar{\nu}$ | 0.1133E+06 | 1.0 | 0.0120 | 48950 | 30 | 0.8 | 0.0278 |
| $pp \rightarrow W^+ W^- \rightarrow \mu^+ \nu \tau^- \bar{\nu}$ | 0.1133E+06 | 1.0 | 0.0120 | 44000 | 8 | 0.2 | 0.0309 |
| $pp \rightarrow W^+ W^- \rightarrow \tau^+ \nu e^- \bar{\nu}$ | 0.1133E+06 | 1.0 | 0.0120 | 47700 | 2 | 0.1 | 0.0285 |
| $pp \rightarrow W^+ W^- \rightarrow \tau^+ \nu \mu^- \bar{\nu}$ | 0.1133E+06 | 1.0 | 0.0120 | 45800 | 8 | 0.2 | 0.0297 |
| $pp \rightarrow W^+ W^- \rightarrow \tau^+ \nu \tau^- \bar{\nu}$ | 0.1133E+06 | 1.0 | 0.0120 | 34850 | 0 | 0.0 | 0.0390 |
| $pp \rightarrow ZZ \rightarrow \ell^+ \ell^- \ell^+ \ell^-$ | 0.1886E+05 | 1.0 | 0.0045 | 35700 | 8597 | 20.4 | 0.0024 |

Table 1. Breakdown of MC samples used for ZW analysis.

[12] *MC@NLO* MC generator (V2.3) by S. Frixione and B. Webber,

<http://www.hep.phy.cam.ac.uk/theory/webber/MCatNLO/>

PYTHIA (v6.3) by T. Sjostrand et al., *Comput. Phys. Commun.*, **135**, (2001) 238259

| Training Variables | Gini Index Contribution(%) | |
|--|----------------------------|-----------------|
| | Event Reweighting | Equal Weighting |
| $P_T(Z \rightarrow \ell^-)$ | 2.41 | 1.46 |
| N_{trk}^{iso} (tracks around $Z \rightarrow \ell^-$ in $\Delta R < 0.4$ cone) | 4.53 | 2.13 |
| $P_T(Z \rightarrow \ell^+)$ | 1.93 | 1.34 |
| N_{trk}^{iso} (tracks around $Z \rightarrow \ell^+$ in $\Delta R < 0.4$ cone) | 7.65 | 2.49 |
| $P_T(W^\pm \rightarrow \ell^\pm)$ | 4.16 | 3.01 |
| $\sum P_T^{iso}$ (tracks around $W^\pm \rightarrow \ell^\pm$ in $\Delta R < 0.4$ cone) | 11.88 | 11.80 |
| N_{trk}^{iso} (tracks around $W^\pm \rightarrow \ell^\pm$ in $\Delta R < 0.4$ cone) | 20.56 | 14.56 |
| $\sum E_T^{iso}$ (jets around $W^\pm \rightarrow \ell^\pm$ in $\Delta R < 0.4$ cone) | 2.07 | 5.83 |
| f_ℓ^{iso} | 2.05 | 4.57 |
| $\Delta A(Z \rightarrow \ell^+, W^\pm \rightarrow \ell^\pm)$ | 3.26 | 2.73 |
| $\Delta R(Z \rightarrow \ell^+, W^\pm \rightarrow \ell^\pm)$ | 2.63 | 2.49 |
| $\Delta A(Z \rightarrow \ell^-, W^\pm \rightarrow \ell^\pm)$ | 4.17 | 3.12 |
| $\Delta R(Z \rightarrow \ell^-, W^\pm \rightarrow \ell^\pm)$ | 3.05 | 3.07 |
| MET -missing transverse energy | 3.90 | 10.26 |
| $P_T(WZ)$ | 1.59 | 3.88 |
| $M_{\ell\ell}$ | 9.70 | 4.22 |
| $M_T(\ell, MET)$ | 7.55 | 6.67 |
| H_t | 0.91 | 0.94 |
| $\sum E_T^{jet}$ | 0.91 | 1.73 |
| E_T^h | 0.72 | 6.03 |
| $MET / \sqrt{\sum_i E_T(i)}$ | 0.95 | 4.10 |
| E_T^{recoil} | 3.42 | 3.58 |

Table 2. Gini index contributions of input variables for BDT training using event reweighting and equal weighting techniques. $Z \rightarrow \ell$ means lepton decays from Z and $W \rightarrow \ell$ means lepton decays from W.

| | | | | | | |
|-------------------------------------|------|------|------|-------|-------|-------|
| N_{signal} | 60 | 80 | 100 | 120 | 140 | 160 |
| N_{bg1} for ANN-equal-weighting | 30.5 | 51.9 | 72.4 | 104.7 | 133.3 | 177.6 |
| N_{bg2} for ANN-event-reweighting | 5.8 | 7.7 | 9.8 | 14.7 | 25.9 | 34.9 |
| $Ratio = N_{bg1}/N_{bg2}$ for ANN | 5.3 | 6.7 | 7.4 | 7.1 | 5.1 | 5.1 |
| N_{bg3} for BDT-equal-weighting | 18.5 | 39.4 | 60.7 | 69.1 | 88.9 | 110.1 |
| N_{bg4} for BDT-event-reweighting | 3.1 | 4.0 | 6.3 | 8.4 | 13.2 | 19.3 |
| $Ratio = N_{bg3}/N_{bg4}$ for BDT | 6.0 | 9.9 | 9.6 | 8.2 | 6.7 | 5.7 |

Table 3. Number of background events (N_{bg}) versus number of signal events (N_{signal}) using the ANN and BDT discriminating algorithms with equal weighting and event reweighting training techniques.

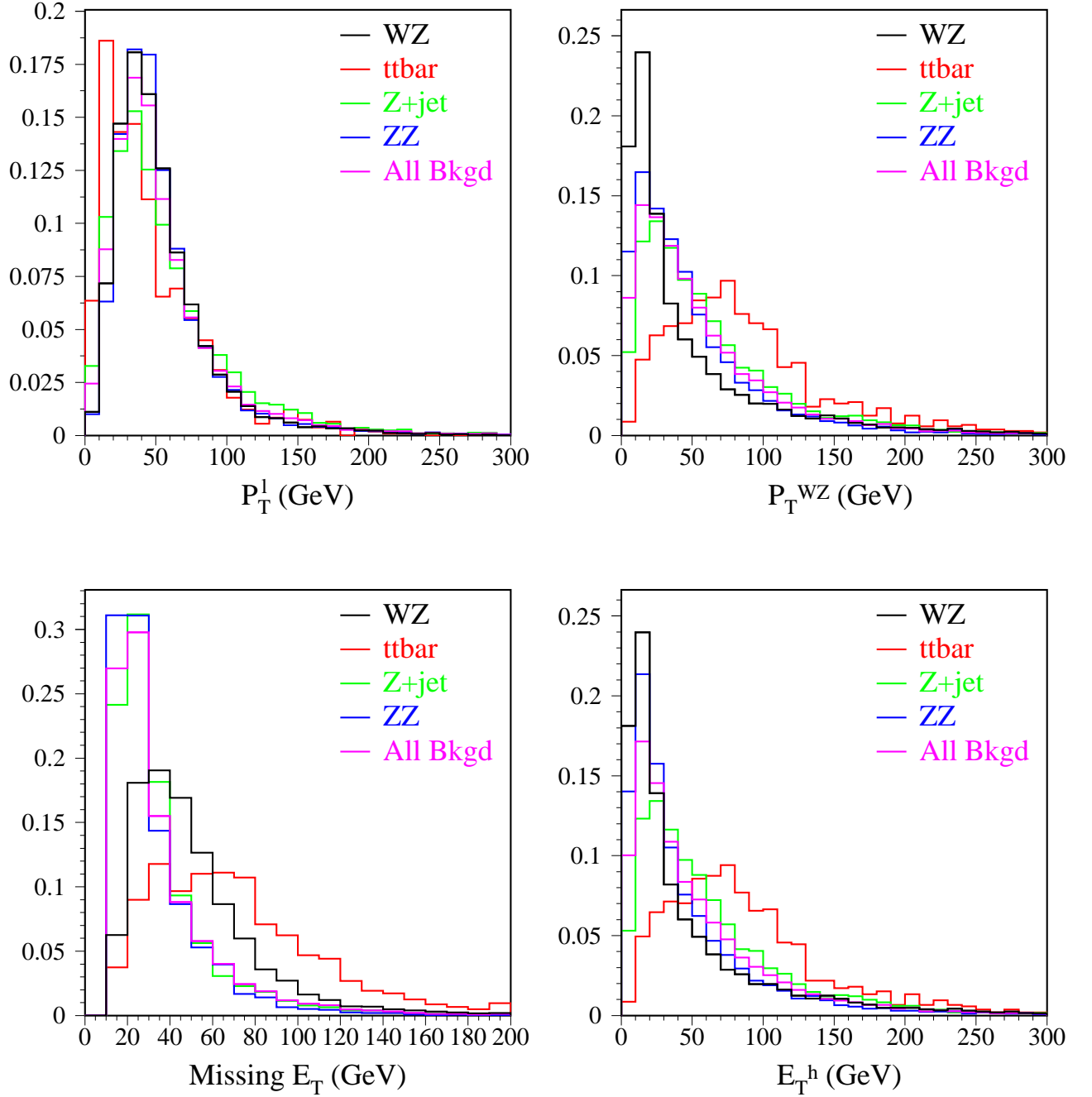


Figure 1. Distributions of the transverse momentum of leptons (top left), the transverse momentum of the WZ system (top right), the missing transverse energy of the event (bottom left) and the vector sum of transverse momenta from leptons and MET (bottom right). Among the histograms, black indicates ZW signal events, red indicates $t\bar{t}$, green indicates Z plus jets, blue indicates $ZZ \rightarrow \ell\ell\ell\ell$ and pink indicates a combination of all backgrounds. All histograms are normalized to the same area for comparison.

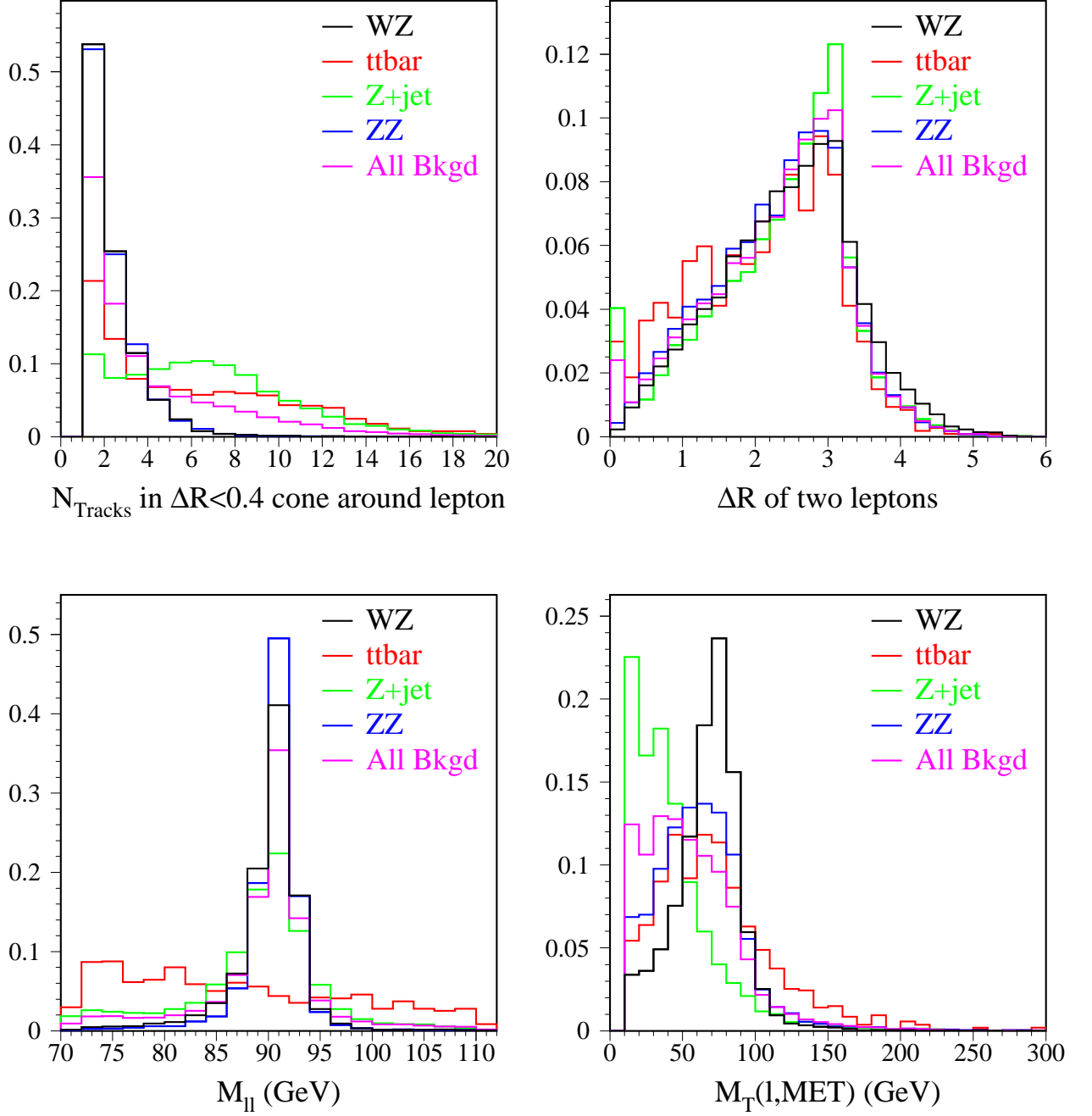


Figure 2. Distributions of the number of charged tracks around a lepton in a cone of $\Delta R = 0.4$ (top left), the two lepton separation in ΔR (top right), the invariant mass of two leptons (bottom left) and the transverse mass of leptons combined with MET (bottom right). Among the histograms, black indicates ZW signal events, red indicates $t\bar{t}$, green indicates Z plus jets, blue indicates $ZZ \rightarrow \ell\ell\ell\ell$ and pink indicates a combination of all backgrounds. All histograms are normalized to the same area for comparison.

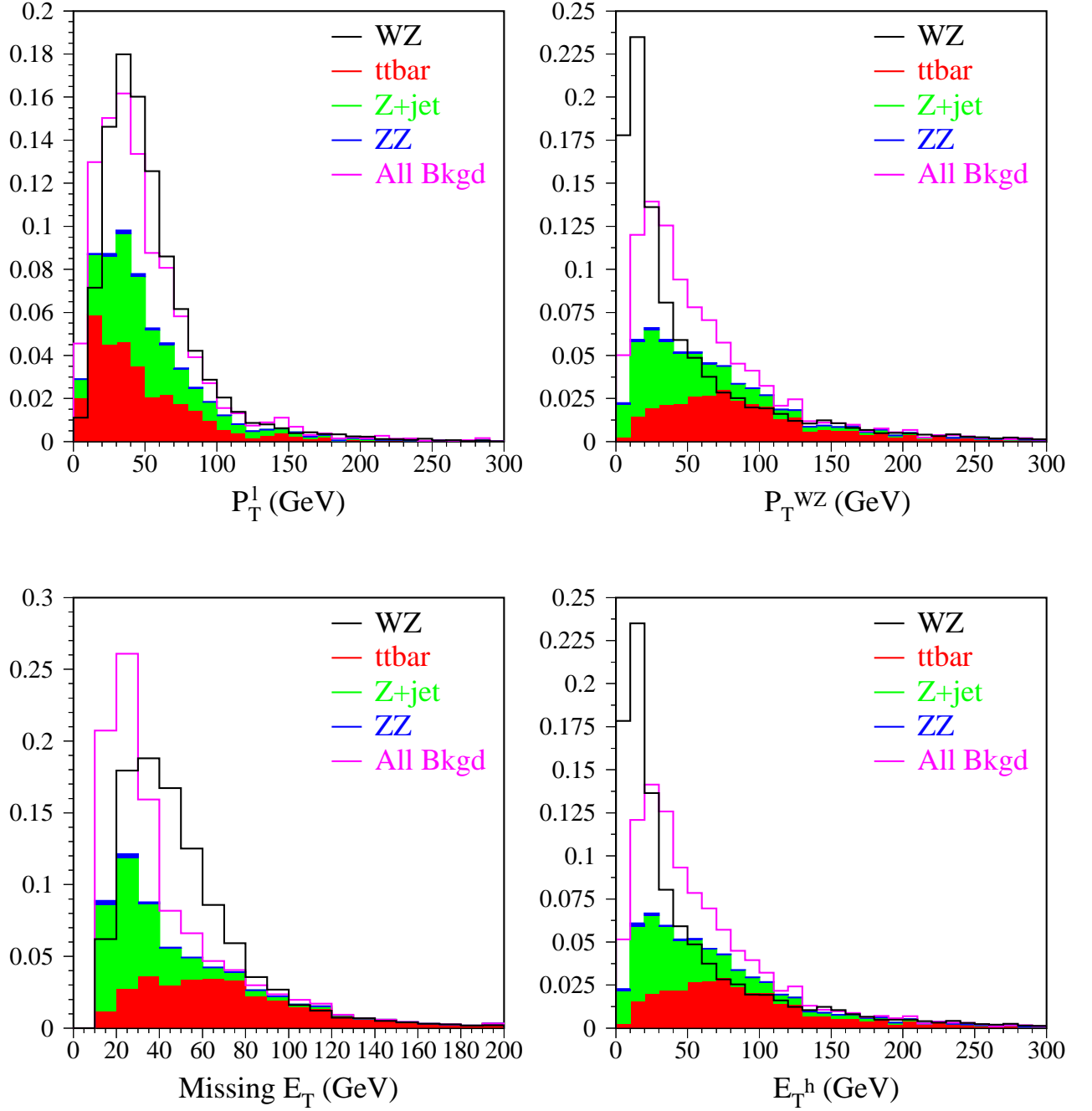


Figure 3. Distributions of the transverse momentum of leptons (top left), the transverse momentum of the WZ system (top right), the missing transverse energy of the event (bottom left) and the vector sum of transverse momenta from leptons and MET (bottom right). Among the histograms, black indicates ZW signal events, red indicates $t\bar{t}$, green indicates Z plus jets, blue indicates $ZZ \rightarrow \ell\ell\ell\ell$ and pink indicates a combination of all backgrounds. Signal and total reweighted background events are normalized to the same area for comparison. Major background are stacked indicating the relative contributions.

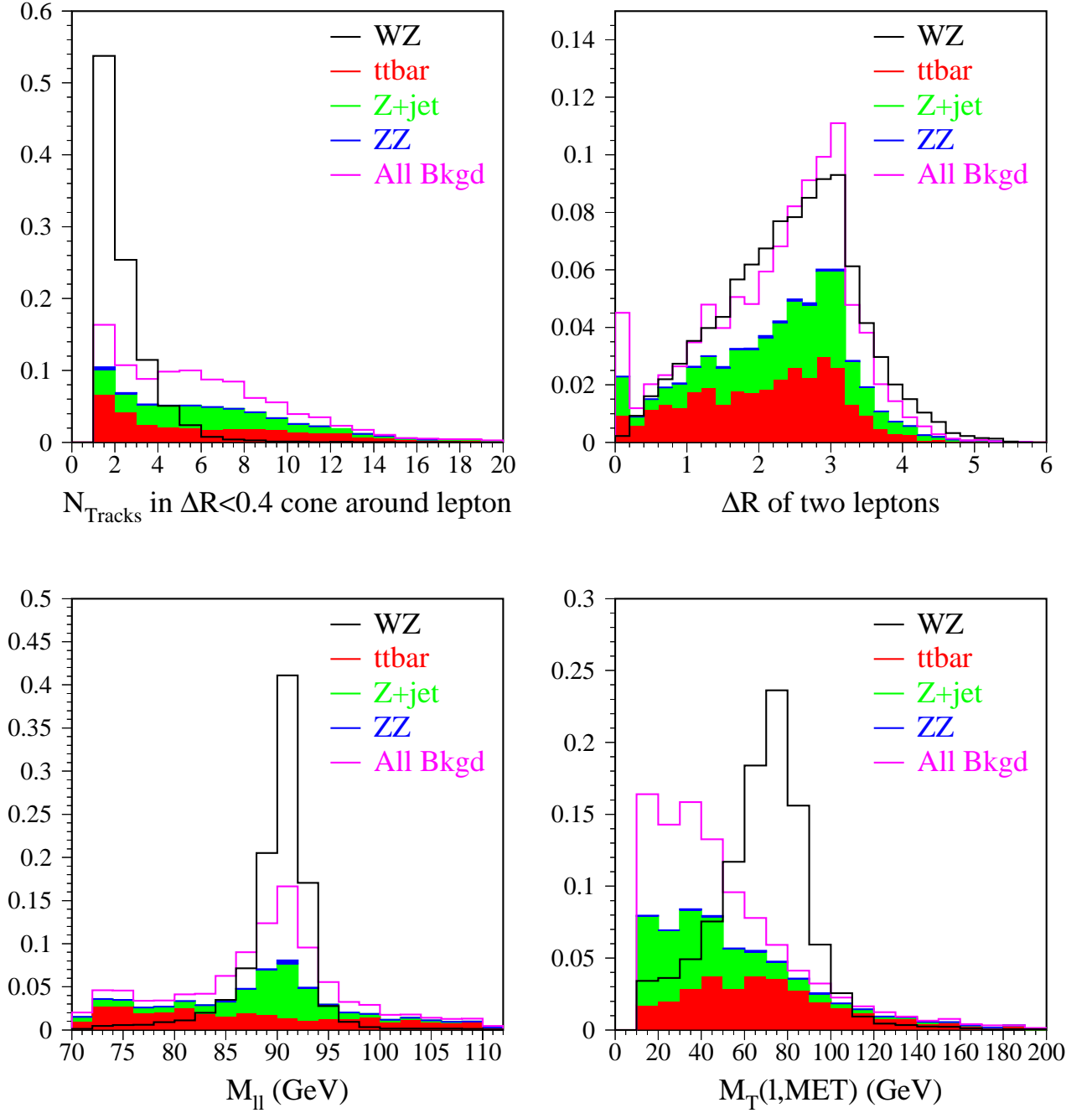


Figure 4. Distributions of the number of charged tracks around a lepton in a cone of $\Delta R = 0.4$ (top left), the two lepton separation in ΔR (top right), the invariant mass of two leptons (bottom left) and the transverse mass of leptons combined with MET (bottom right). Among the histograms, black indicates ZW signal events, red indicates $t\bar{t}$, green indicates Z plus jets, blue indicates $ZZ \rightarrow \ell\ell\ell\ell$ and pink indicates a combination of all backgrounds. Signal and total reweighted background events are normalized to the same area for comparison. Major background are stacked indicating the relative contributions.

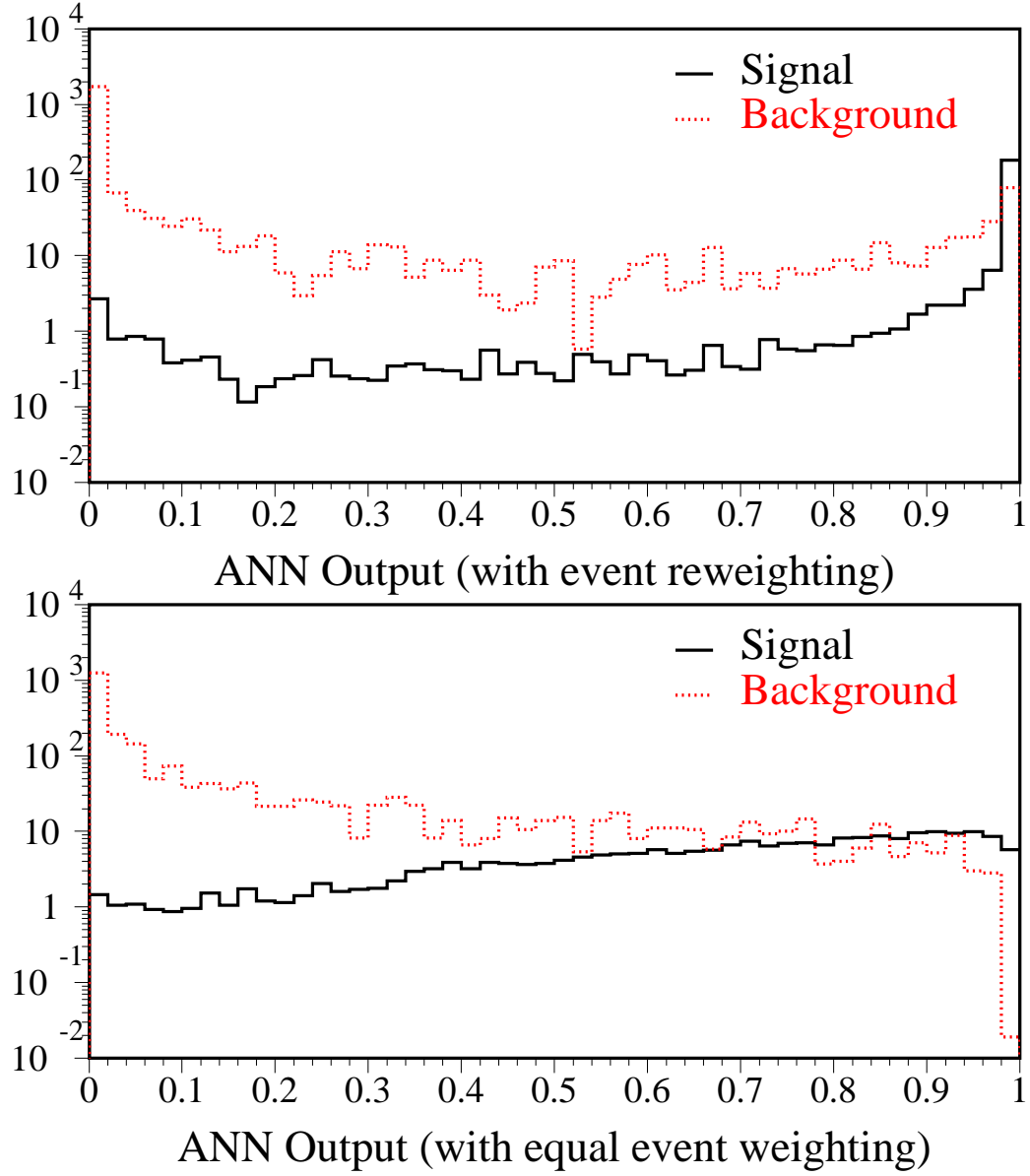


Figure 5. Distributions of the ANN output for testing samples assuming integrated luminosity of 1 fb^{-1} .

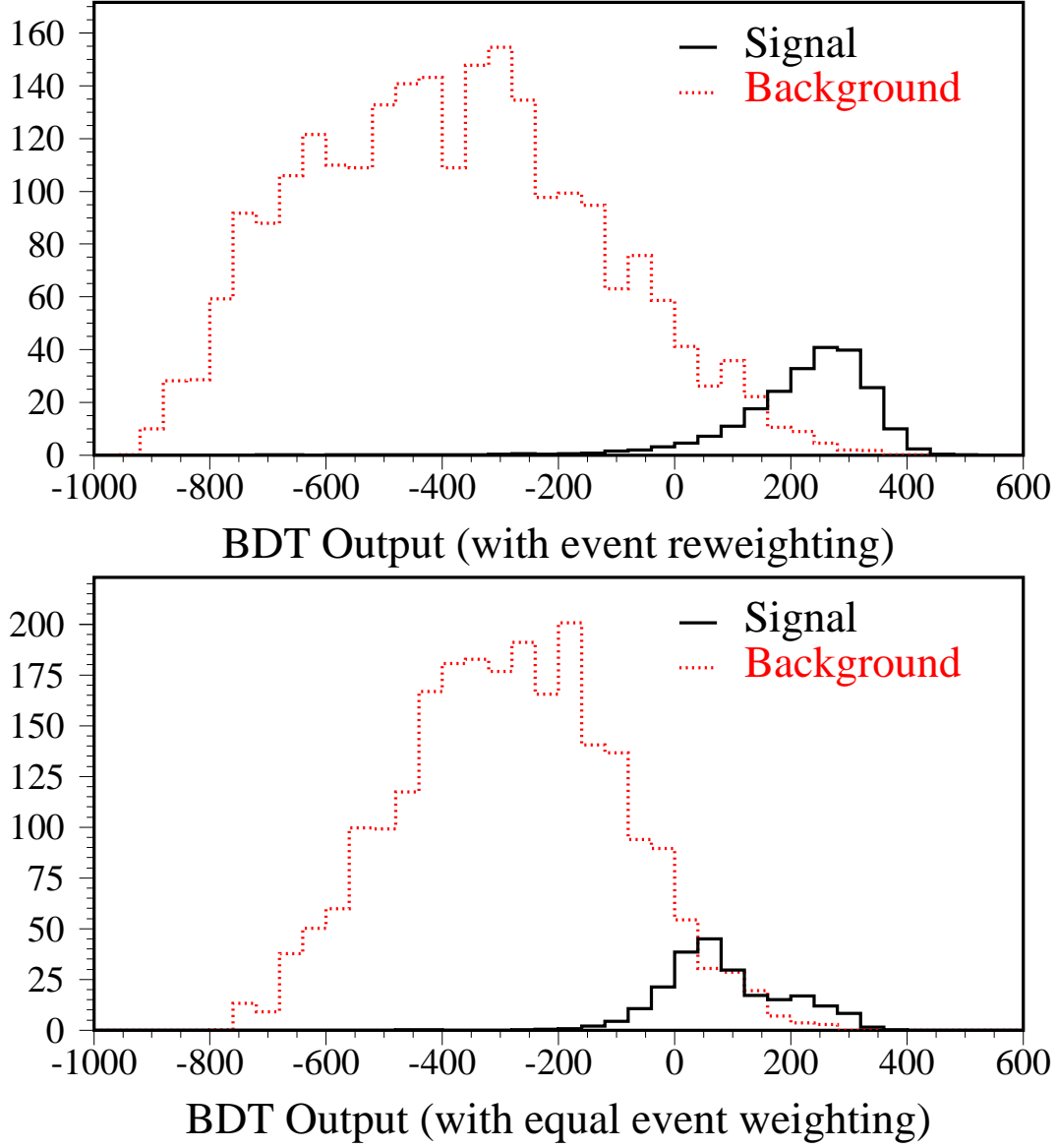


Figure 6. Distributions of the BDT output for testing samples assuming integrated luminosity of 1 fb^{-1} .

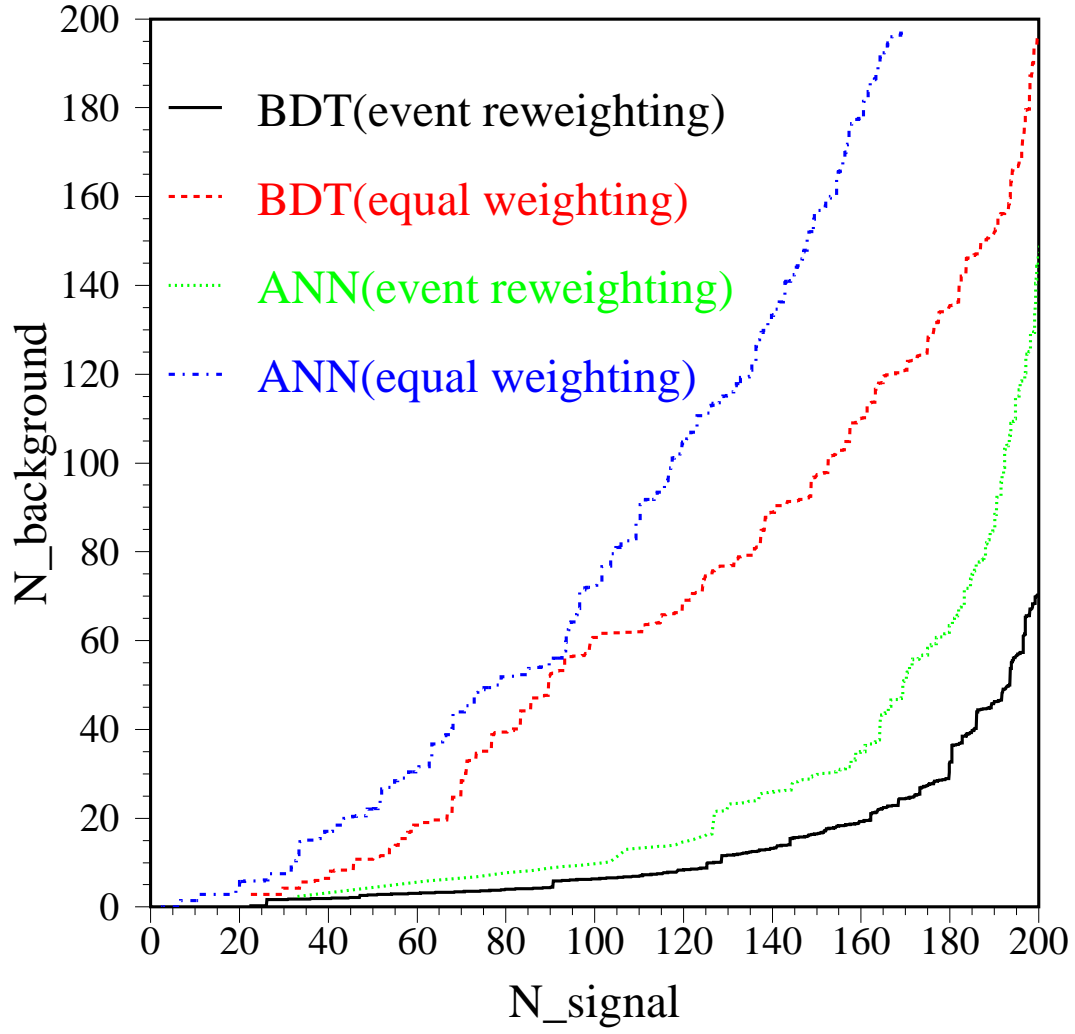


Figure 7. Number of background events versus number of signal events for testing samples assuming integrated luminosity of 1 fb^{-1} .

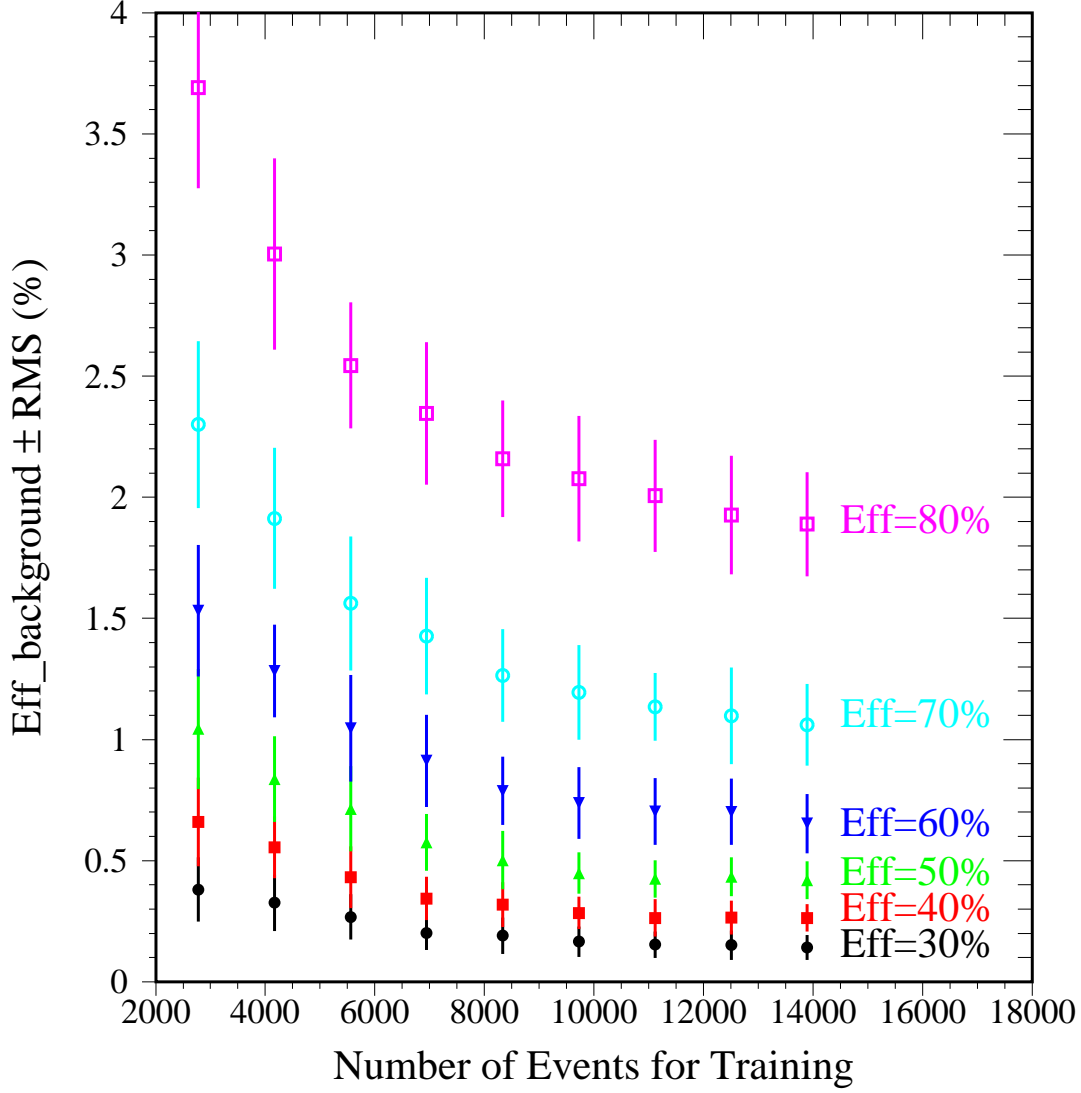


Figure 8. Background efficiencies versus number of training events for various signal efficiencies. Training events are selected randomly but the testing sample is fixed for the comparison. The BDT training-testing process is repeated 50 times to obtain average background efficiencies and RMS for a set of fixed signal efficiencies.